07

Plastic flow in Cu-Ni solid solutions as an autowave process

© S.A. Barannikova, L.B. Zuev, M.V. Nadezhkin

Institute of Strength Physics and Materials Science, Siberian Branch, Russian Academy of Sciences, Tomsk, Russia

E-mail: lbz@ispms.ru

Received June 22, 2022
Revised January 10, 2023
Accepted January 12, 2023

The influence of Ni content in Cu-Ni alloys on the localization of plastic flow under uniaxial tension has been studied. The regularities of localization of plastic deformation during linear and parabolic deformation hardening, as well as at the yield point, depending on the Ni content in the solid solution, have been studied by the speckle photography method. The influence of the Ni content on the duration of the stages of parabolic deformation hardening in alloys of different composition was found. The dependence of the spatial period of localization of plastic deformation (the length of the localization autowave) on the Ni content in the studied alloys is established.

Keywords: localization of plastic deformation, autowaves, copper-nickel alloys, structure, mechanical properties, deformation and impurity hardening.

DOI: 10.21883/PSS.2023.03.55586.412

1. Introduction

Physics of plastic flow in solids, despite the huge volume of research performed by now, is still far from its completion [1]. The most complicated problems that researchers are faced with are the nature of multiscale character of the processes typical for different aspects of the plasticity phenomenon and description of this nature. For example, it is difficult to match the dislocation scale defined by the Burgers vector of dislocation, which is $b \approx 10^{-10}$ m, and the typical scale of strain localization of $\sim 10^{-3}-10^{-2}$ m. It is already clear now that this and many other challenges in the physics of plasticity can not be understood and explained without taking into account nonlinearity, activity and nonequilibrium state of deforming media [2,3]. However, the few attempts to take into account these properties made models considerably more complicated and almost did not go any further in the existing approaches to the problem of plasticity.

Some progress has become visible within the autowave approach to the physics of plastic flow, which is developing now [4–7]. It is based on the idea that plastic deformation is a macroscopically localized process of self-organization of defect ensembles initiated by nonlinearity and activity of a nonequilibrium deforming medium. This hypothesis was validated by experiments with monocrystalline and polycrystalline metals and alloys, which are deformed due to dislocation gliding, twinning or deformation-induced phase transformation [4–7]. According to this approach, the systems of active plastic flow nuclei evolving in the process of deformation are interpreted as autowave processes (modes), which are characterized by a scale of $5 \cdot 10^{-3} \leq \lambda \leq 1.5 \cdot 10^{-2}$ m an a propagation speed of $10^{-5} \leq V_{aw} \leq 10^{-4}$ m/s. It's important to notice that autowave modes change following the change in the work hardening characteristic. Based on these ideas many patterns of plastic flow in materials of different nature can be satisfactorily described [7].

Themajor portion of basic experiments of the autowave theory was made earlier in conditions when only forms of the work hardening characteristic or mechanisms of dislocation deformation were changed in the material under study [7]. On this background, almost full absence of information about autowave processes of deformation at different levels of impurity hardening looks as an embarrassing shortage, the more so as there is a direct proof of existence of the effects, which is related to the influence of nitrogen interstitial atoms on characteristics of plastic deformation autowaves in chrome-nickel austenite monocrystals [7].

This study is aimed to get rid of this gap. It is focused on studying the character of localized plasticity autowave development in alloys, where solid-solution hardening plays an important role [8]. This goal should be achieved through the planned comparison of localized plasticity autowave development in alloys with different level of impurity hardening, however with the same mechanism of work hardening.

2. Material specifications. Research methods

The stated goal was achieved through studying the autowave characteristics of plastic deformation localization in Cu-Ni alloys, which are different from each other by the content of Ni in the range of $\sim 2-60$ at.% (see Table 1). As it is known [8], this alloy system features a continuous series of FCC solid solutions based on copper with different physical and mechanical properties but close microstructures and hardening mechanisms.

Table 1. Chemical composition of studied alloys

Alloy	Notation in the text	Content of impurities, at.%	
		Ni	Mn
Manganin	**1**	4.34	16.09
Cupronickel	**2**	19.61	–
Constantan	**3**	40.04	1.99
Monel	**4**	64.02	0.3

To characterize the alloys under study, first we have checked them for fulfilment of Vegard's law [9] that predicts the linear relation between the lattice parameter and the content of alloying element (Ni). Parameters of crystal lattice of FCC solid solutions were determined using a DRON-7 X-ray diffractometer („NANOTECH" Research Equipment Sharing Center of the Institute of Strength Physics and Materials Science of the Siberian Branch of the Russian Academy of Sciences) with the use of CoKα radiation with an accuracy of $\sim 10^{-3}$ nm. Scanning points were spaced with an interval of 0.05° (for general review diffraction pattern) and 0.02° (for far angles — to refine the lattice parameter), accumulation times in every point were 3 and 10 s, respectively, in the angular range of $2\Theta = 20-160°$. Phases were indicated by comparing diffraction peak positions with the information from the JCPDS database. Fig. 1 confirms fulfilment of Vegard's law in the Cu-Ni alloys under study. This curve was built with the position of point 1 for alloy **1** with increased content of Mn corrected by calculation on an assumption of additive and linear contributions of size effects from Ni and Mn [8,9]. It was taken into account that effects of Ni and Mn impurities on the Cu lattice parameter have opposite signs because $a_{Ni} < a_{Cu}$, but $a_{Mn} > a_{Cu}$. By assuming appropriate contributions additive, an equivalent concentration of impurities can be evaluated for the given alloy, as shown in Fig. 1.

Microstructure of alloys **1**–**4** was observed by metallographic method using a Neophot-21 microscope. The procedure of metallographic specimen preparation included mechanical grinding and polishing. Grain boundaries were identified by etching with the following reagent: 100 ml of 0.4%-th $KMnO_4$ + 10 ml of H_2SO_4. Grain sizes of all alloys were close to each other and were in the range from 65 to 110 μm.

Dumbbell specimens for mechanical tests with a working part size of $50 \times 10 \times 2$ mm were stamped from rolled and annealed sheets. Diagrams of plastic flow in stress σ–strain ε coordinates were recorded at uniaxial tension of specimens in a Walter + Bai LFM-125 machine at 300 K and a movable grip speed of 0.2 mm/min, which was corresponding to a deformation rate of $6.7 \cdot 10^{-5}$ s^{-1}.

The information presented in Fig. 2 and in Table 2 shows that the increase in Ni content leads to an increase in tensile strength of Cu-Ni alloys almost without decrease in their plasticity. An exception was alloy **1** where Mn content exceeded Ni content.

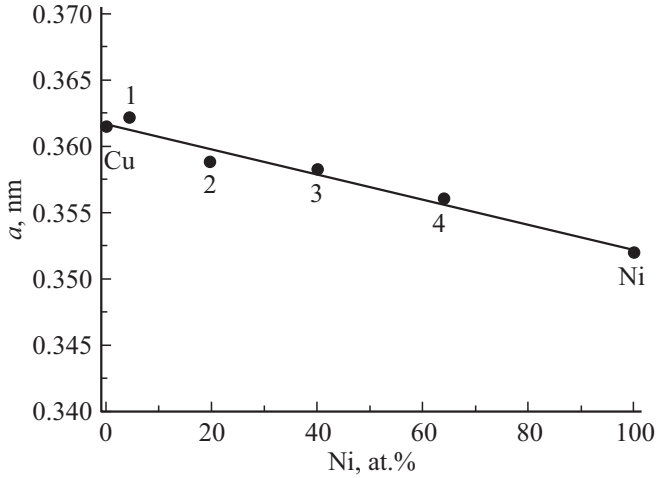

Figure 1. Crystal lattice parameter as a function of Ni content for alloys **1**–**4**

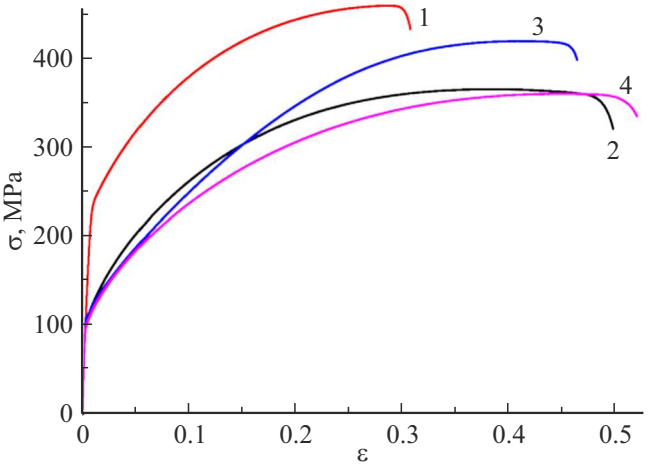

Figure 2. Stress-strain curves of alloys **1**–**4**.

Alloying changes the form of work hardening coefficient dependence on deformation $d\sigma/d\varepsilon = \theta(\varepsilon)$. A common feature for all investigated alloys is the presence of the stage of parabolic work hardening ($\theta \sim \varepsilon^{-1/2}$) in curves of $\sigma(\varepsilon)$. With growth of Ni content this stage starts at a greater deformations and becomes shorter (see Table 2). The stage of parabolic work hardening in curves of all alloys is followed by a prefailure stage, which precedes the failure neck formation.

Mechanical tests of alloys were supplemented by *in situ* analysis of localized plasticity pattern geometry, which arises in the specimens under deformation. The analysis was performed using a ALMEC-*tv* laser measuring complex [10]. It is intended to reconstruct displacements vector fields under the deformation using methods of digital image correlation (DIC) and digital static speckle photography (DSSP).

Table 2. Staging of plastic flow and mechanical characteristics of studied alloys

Alloy	Duration of observed stages of the work hardening			Mechanical characteristics		
	yield plateau	linear	parabolic	σ_y, MPa	σ_B, MPa	δ, %
Cu	–	0.05–0.2	0.21–0.38	0.4–0.52	55.0 ± 2.6	310.0 ± 3.8
1	–	0.04–0.17	0.18–0.28	230.0 ± 3.0	462.0 ± 5.0	31.3 ± 0.3
2	–	0.04–0.23	0.24–0.35	85.0 ± 2.5	362.0 ± 4.0	48.0 ± 2.0
3	0.04–0.06	0.02–0.3	0.33–0.41	110.0 ± 2.0	423.0 ± 4.0	47.4 ± 0.8
4	–	0.03–0.36	0.37–0.4	105.0 ± 2.5	363.0 ± 4.0	49.0 ± 3.2
Ni	–	–	0.04–0.37	0.38–0.51	70.0 ± 2.6	460.0 ± 3.5

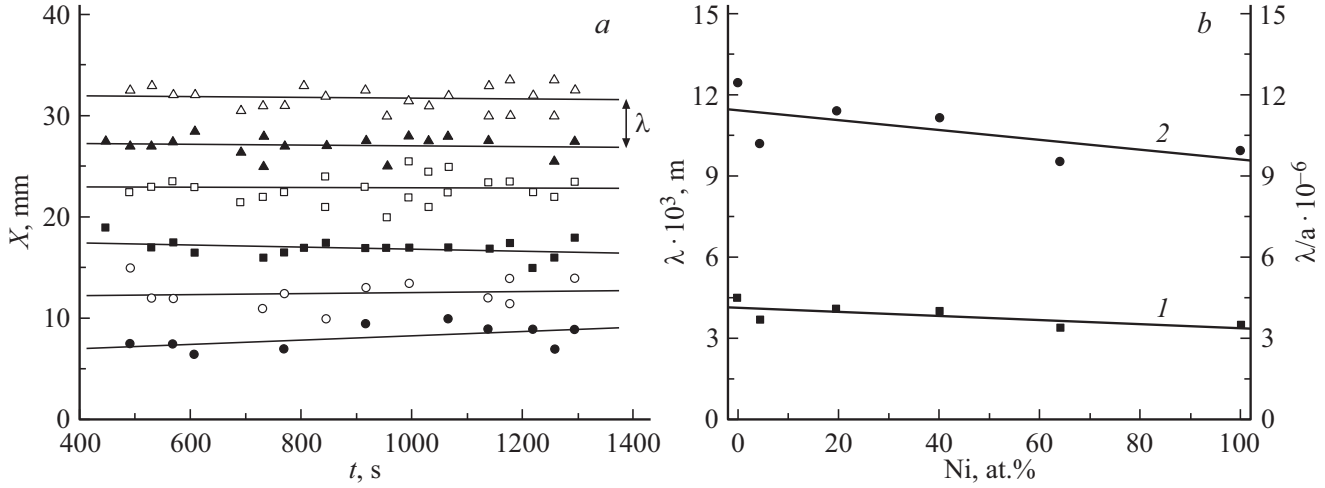

Figure 3. $X-t$ diagram of distribution of local elongations ε_{xx} at the parabolic stage of work hardening for alloy **1** (a); autowave length at this stage in alloys **1**–**4** (b). Straight line *2* is for λ; straight line *1* is for λ/a.

This allowed recording the pattern of localized plasticity and monitoring the development of plastic flow localization zones by processing the quantitative information on the distribution of plastic distortion tensor components over the deformed specimen and their evolution in time. For the analysis, space-time distributions of local deformations (dependencies of positions of maxima of the local elongation component ε_{xx} on the coordinate along the axis of tension or on time) were plotted. These distributions contain information on motion speeds, spatial and temporal periods of the evolution of localization zone deformation.

The technique used supplements the information on mechanical properties of the metal with the geometry of localized plasticity pattern. This makes it possible to relate force characteristics of the flow process to the information on localization of the deformation and gain a deeper understanding of the autowave nature of plastic flow.

3. Autowave patterns of plastic flow of Cu-Ni alloys

It follows from the above that to find out the effect of alloying degree of an alloy on its deformation parameters, it is reasonable to compare the patterns typical for localization at the stage of parabolic work hardening, a typical stage of all the alloys under study. In the course of experiments it has been found that for alloys **1**–**4** at a deformation in these conditions the distributions of ε_{xx} component over the specimen, as shown in Fig. 3, a, form an ordered system of equidistant stationary localization nuclei, which is characterized by a spatial period (autowave length) of $\lambda = (3-4.5) \pm 1$ mm. In terms of autowave theory systems like this correspond to stationary dissipative structures. They are usual for all materials that have their flow curve with a parabolic stage [6,7]. It follows from Fig. 3, b that autowave length λ in this case is almost independent on the content

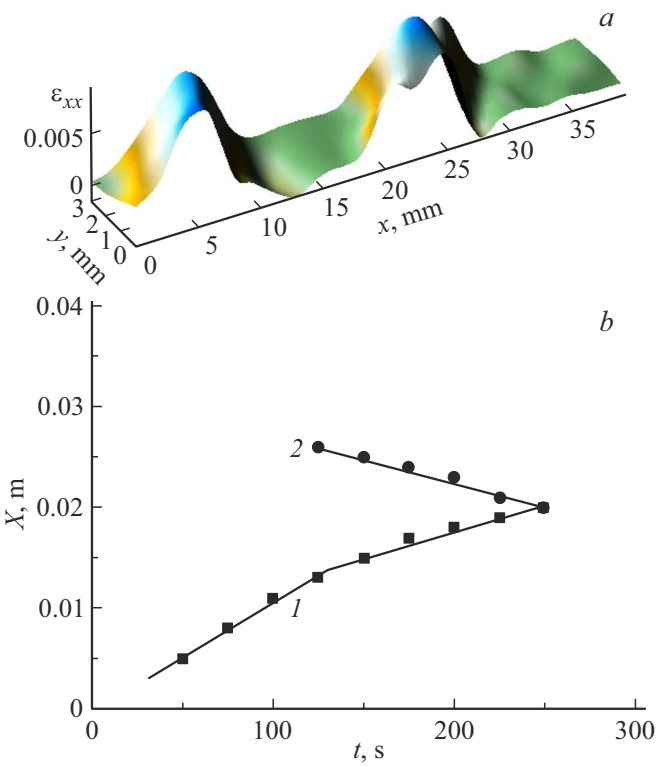

Figure 4. Localization of plastic deformation on the yield plateau for alloy **3**: distribution of local elongations ε_{xx} (a); kinetic diagram of countermotion of Lüders fronts (b).

of Ni, however the dimensionless autowave length λ/a decreases linearly with growth of the Ni content.

As is clear from Table 2, in alloy **3** the existence of yield plateau ($\theta = 0$) and linear work hardening ($\theta = \text{const} > 0$) stages is additionally noted before the parabolic hardening. In these cases autowave modes are generated in the deforming medium, which are different from the described stationary dissipative structures, but typical for the same stages of deformation of other materials [4,5].

Thus, the plastic flow localization is manifested at the yield plateau as a nucleation and expansion of the Lüders bands, on which fronts the deforming medium is irreversibly transits from elastic to plastic state [11]. With the observed configuration of bands and fronts, there is an area in the central part of the specimen where two Lüders fronts move opposite to each other (Fig. 4, a). The information about meeting of the fronts obtained from the analysis of the $X-t$ diagram of their motion shown in Fig. 4, b suggests that in the beginning the distributions of deformation fronts correspond to the Lüders band (1) nucleated at the fixed grip of the test machine. Front of this band was moving from the fixed grip at a speed of $\sim 5.5 \cdot 10^{-4}$ m/s. Then, near the movable grip, the second Lüders band (2) has been nucleated. One of its fronts was moving towards the first front with the same speed. When this front has arisen, the speed of earlier arisen front has decreased about two times. At the moment of their meeting the fronts have annihilated and the yield plateau has ended up.

Autowave effects of alloy **3** deformation within the yield plateau are completely correspondent to the patterns determined for the Lüders deformation in iron and titanium nickelide and described in [12]. This study gives a general explanation of the deformation process within the yield plateau, which, in this case, is related to the development of a switching autowave [7], taking the form of moving front of the Lüders band in these conditions.

At the stage of linear work hardening in alloy **3** a phase autowave of the localized plasticity was observed with a length of ~ 5 mm and a propagation speed of $\sim 2 \cdot 10^{-4}$ m/s. These characteristics are fully consistent with appropriate parameters determined for deformation of other materials at the stage of linear work hardening.

Thus, the autowave modes of localized plasticity found in Cu-Ni alloys are completely consistent in their form with the modes observed in other materials at the same stages of hardening [4–7]. The different alloying levels in alloys **1**–**4** has only caused a difference in quantitative characteristics of the observed autowaves, despite the large range of Ni concentrations used. Thus, the experiments confirm one of the basic statements of the autowave theory of plasticity — *the Correspondence Rule* [6,7], which argues that each form of work hardening pattern corresponds to a certain autowave mode of plastic flow: *a switching autowave* at the yield plateau, *a phase autowave* and *a stationary dissipative structure* at the stages of linear and parabolic work hardening, respectively.

4. Autowave criterion of plasticity for deformations of Cu-Ni alloys

As it was shown in [4–7], for phase autowaves of localized plasticity arising at the stage of linear work hardening the following invariant relationship is valid:

$$\frac{\lambda V_{aw}}{\chi V_t} = \hat{Z} \approx \frac{1}{2}, \qquad (1)$$

where $\chi \approx a$ is interplanar distance of the deforming material, and V_t is the propagation speed of transverse ultrasonic waves in this material. Equation (1) establishes a relation between characteristics of localized plasticity autowave propagation (numerator) and characteristics of elastic waves (denominator) and is considered as the basic equation of the autowave theory of plasticity [6,7]. Numerous consequences derived from equation (1) describe qualitatively and quantitatively many patterns of the plastic flow [5]. In addition, the product of (λV_{aw}) with a dimension of $\text{m}^2 \cdot \text{s}^{-1}$ characterizes stability of the deformation process at the stage of linear work hardening, where plasticity zones move uniformly over the specimen providing equal deformations in all its cross-sections. This parameter can serve a convenient criterion (index) of plasticity [7].

Table 3. Calculated and experimental estimations of the plasticity parameter

Metal	χ	θ_D	$()\lambda V_{aw}^{(\text{calc})}$	$(\lambda V_{aw})^{\text{exp}}$	$(\lambda V_{aw})^{(\text{calc})}/(\lambda V_{aw})^{(\text{exp})}$
	$\times 10^{10}$, m	K	$\times 10^7$ m^2/s		
Ni	2.03	375	1.6	2.1	0.8
Cu	2.08	315	1.4	3.6	0.4
Al	2.33	394	2.2	2.6	0.8
Mo	2.22	380	1.9	1.2	1.6
Co	2.18	385	1.9	1.3	1.5
Sn	3.75	170	2.5	2.4	1.0
□-Fe	2.02	420	1.8	2.55	0.7
In	2.72	129	0.95	2.6	0.4
Zn	2.08	234	1.0	3.7	0.3
Cd	2.34	120	0.65	0.9	0.7
Mg	2.45	318	1.9	9.9	0.2

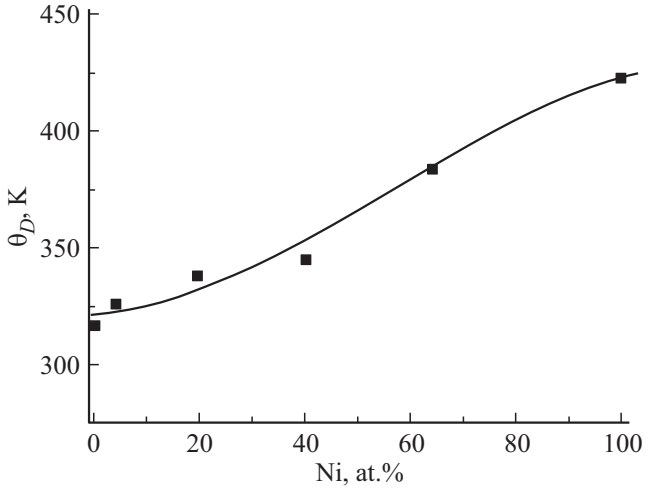

Figure 5. Debye temperature as a function of Ni content in Cu-Ni alloys (according to [14]).

The important role of invariant (1) in the autowave theory of plasticity requires to discuss the possibility of its application for the parabolic stage of work hardening. The difficulty is related to the fact that a stationary dissipative structure with $V_{aw} = 0$ is formed at this stage. By applying the relationships of $V_t \approx 2\chi(\omega_D/2\pi)$ and $\hbar\omega_D \approx D_B\theta_D$ [13], we reduce equation (1) to the following form:

$$(\lambda V_{aw})^{(\text{calc})} \approx \frac{k_B}{2\hbar} \cdot \left(\chi^2\theta_D\right). \qquad (2)$$

Here ω_D and θ_D are Debye frequency and Debye constant (Debye temperature), while k_B and $\hbar = h/2\pi$ are Boltzmann constant and Plank constant, respectively.

It follows from equation (2) that the plasticity criterion (λV_{aw}) is completely defined by the lattice characteristics χ and θ_D of the alloy. This important fact allows for the direct verification, in the course of which calculations were performed by equation (2) for a number of metals with reliably determined Debye parameters θ_D [13] (Table 3). They were compared with experimentally obtained values for this parameter [7]. Mean ratio of calculated and experimentally obtained values of $(\lambda V_{aw})^{(\text{calc})}/(\lambda V_{aw})^{(\text{exp})}$ was ~ 0.8. This estimation suggests the possibility to apply equation (2) for qualitative estimations of the plasticity criterion (λV_{aw}).

To estimate the effect of Ni concentration on the (λV_{aw}) criterion, we can use the dependence of $a \approx \chi$ on Ni concentration that is obtained experimentally in this study (Fig. 1) and the same dependence of Debye parameter θ_D (Fig. 5) taken from [14]. Corresponding concentration dependence of $k_B/2\hbar \cdot (\chi^2\theta_D)$ in alloys **1**–**4** is shown in Fig. 6, *a*.

Let us compare this result with the dependence of autowave length on Ni content in the alloy (Fig. 3, *b*), as shown in Fig. 6, *b*.

Then, using equation (2), we can formally introduce an effective speed of localized plasticity autowave for the stage of parabolic work hardening as follows:

$$V_{aw}^{(eff)} = \frac{(\lambda V_{aw})}{\lambda} \approx \frac{k_B}{2\hbar} \cdot \left(\chi^2\theta_D\right)\frac{1}{\lambda} \neq 0. \qquad (3)$$

In this relationship λ is an experimentally determined autowave length taken from Fig. 3, *b*. The estimate calculation shows that in this case $V_{aw}^{(eff)} \approx (1.5 \pm 0.1) \cdot 10^{-3}$ m/s. This speed can be given a certain physical meaning for the case of parabolic work hardening and formation of stationary

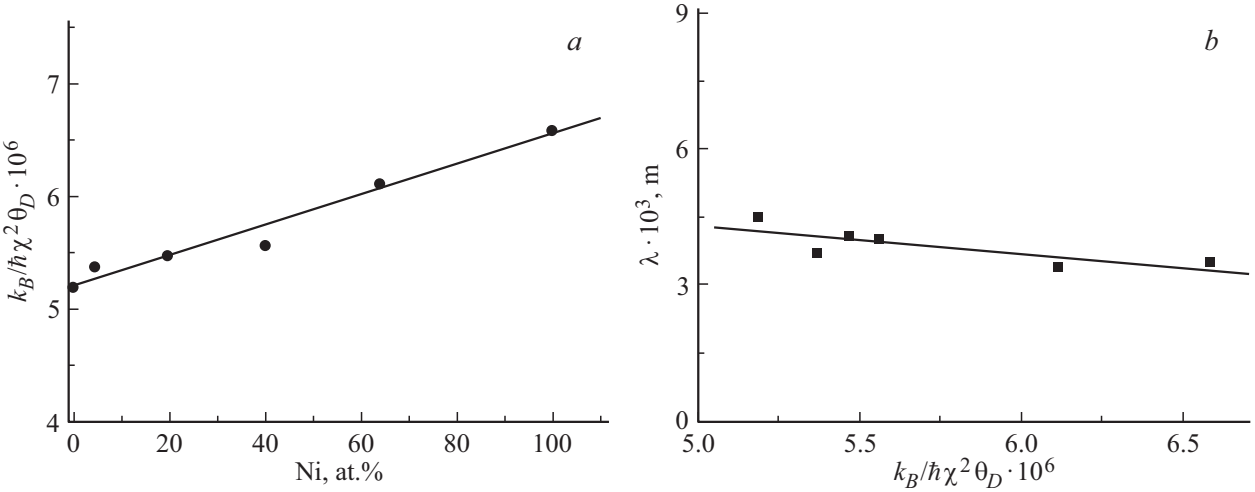

Figure 6. To the estimation of plasticity parameter using relationship (2). Concentration dependence of $k_B/2\hbar \cdot (\chi^2\theta_D)$ (*a*), dependence of autowave length on $k_B/2\hbar \cdot (\chi^2\theta_D)$ (*b*).

dissipative structure. This can be done in a formal way as follows.

It is clear that the displacement of boundaries of the actively deforming area, which is described by the speed V_{aw}, means involvement of new volumes of the material into the process of deformation, as it is typical for the case of linear work hardening. In the case of parabolic work hardening boundaries of the deformation area are not displaced, and the increase in deformation inside the active plastic flow nucleus is probably due to the increase in density of defects in it without macroscopic displacement of deformation localization nuclei boundaries.

The rate of deformation increase in this case is $\dot{\varepsilon} \approx \varepsilon_{xx}/t_c$, where t_c being interframe gap. This allows for introduction of effective autowave speed for the case of parabolic work hardening in the following form:

$$V_{aw}^{(eff)} \approx \frac{\varepsilon_{xx} l}{t_c}. \qquad (4)$$

This speed characterizes in a formal way the development of deformation process in the nucleus of localized plastic flow at the stage of parabolic work hardening. The calculation of $V_{aw}^{(eff)}$ by equation (4) for the conditions of described experiments, that is at $\varepsilon \approx 4 \cdot 10^{-3}$, $t_c \approx 0.1$ s and a specimen length of $l = 5 \cdot 10^{-2}$ m, gives us $V_{aw}^{(eff)} \approx 2 \cdot 10^{-3}$ m/s, which is close to the estimate obtained above using equation (3). This coincidence allows for the suggestion that the elastic-plastic invariant in the form of equation (1) [5,7] can be applied also to the stage of parabolic work hardening.

5. Conclusion

This study, by the example of Cu-Ni alloys, has found that in the case of plastic deformation of impurity-hardened solid solutions autowave modes of localized plasticity observed at the deformation, as in the case of deformation of pure metals, are defined by the patterns of work hardening applicable at the given stage of the process. The most important result is the discovered linearity of dependencies of autowave development parameters of deformation localized plasticity autowaves on the content of nickel in the solid solution. It turned out that Vegard's law is valid in the Cu-Ni system. In addition, the length of the localized deformation autowave at the stage of parabolic work hardening and the autowave plasticity criterion are linear in term of nickel content in the alloy.

It can be said that autowave characteristics of the deformation process „sense" directly the changes in the crystal lattice parameter arising due to alloying. A statement like this makes it possible to establish a relationship between the microscopic theory of impurity hardening [8] and the macroscopic autowave characteristics of deformation processes, thus to find a way to match spatial scales of these phenomena.

Funding

The study was performed as part of the state assignment of the Institute of Strength Physics and Materials Science of the Siberian Branch of the Russian Academy of Science, subject No. FWRW-2021-0011.

Conflict of interest

The authors declare that they have no conflict of interest.

References

[1] G. Grimwall, B. Magyari-Köpe, V. Ozoliņš, K.A. Persson. Rev. Mod. Phys. **84**, 945 (2012).
[2] G.A. Malygin. FTT, **64**, 255 (2022). (in Russian).
[3] A. Zibelewicz. Crystals **10**, 212 (2020).

[4] L.B. Zuev, S.A. Barannikova. Crystals **9**, 458 (2019).
[5] L.B. Zuev, S.A. Barannikova, V.I. Danilov, V.V. Gorbatenko. Prog. Phys. Met. **22**, 3 (2021).
[6] L.B. Zuev, Yu.A. Khon. Phiz. mezomekh.**24**, 5 (2021). (in Russian).
[7] L.B. Zuev. Avtovolnovaya plastichnost. Lokalizatsiya i kollektivnye mody. Fizmatlit, M. (2018). 207 p. (in Russian).
[8] J. Pelleg. Mechanical Properties of Materials. Springer, Dordrecht (2013). 634 p.
[9] J. Christian. Teoriya prevrashcheniy v metallakh i splavakh (in Russian). Mir, M. (1978). 806 p. (in Russian).
[10] L.B. Zuev, V.V. Gorbatenko, K.V. Pavlichev. Measur. Sci. Technol. **21**, 054014 (2010).
[11] Yu.V. Petrov, I.N. Borodin. FTT, **57**, 336 (2015). (in Russian).
[12] L.B. Zuev, V.I. Danilov. FTT, **64**, 1006 (2022). (in Russian).
[13] R.E. Newnham. Properties of Materials. University Press, Oxford (2005). 378 p.
[14] D.H. Timbers. The Debye Temperature and Hardness of Copper-Nickel Alloys. University of Alberta, Edmonton (1964). 146 p.

Translated by Y.Alekseev